SciForschen
Open HUB for Scientific Research

ISSN: 2470-3206

International Journal of Nanomedicine and Nanosurgery

Research Article | Volume: 2.3 | Open Access

Quantitative Evaluation of Tumor Response to combination of Magnetic Hyperthermia Treatment and Radiation Therapy using Magnetic Particle Imaging

Akiko Ohki, Tomomi Kuboyabu, Marina Aoki, Mikiko Yamawaki and Kenya Murase*

Department of Medical Physics and Engineering, Division of Medical Technology and Science, Faculty of Health Science, Graduate School of Medicine, Osaka University, Suita, Osaka, Japan

***Corresponding author:** Kenya Murase, PhD, Department of Medical Physics and Engineering, Division of Medical Technology and Science, Faculty of Health Science, Graduate School of Medicine, Osaka University 1-7 Yamadaoka, Suita, Osaka 565-0871, Japan, Tel & Fax: (81)-6-6879-2571; **E-mail:** murase@sahs.med.osaka-u.ac.jp

Received date: 11 Jul 2016; **Accepted date:** 03 Aug 2016; **Published date:** 09 Aug 2016.

Citation: Ohki A, Kuboyabu T, Aoki M, Yamawaki M, Murase K (2016) Quantitative Evaluation of Tumor Response to combination of Magnetic Hyperthermia Treatment and Radiation Therapy using Magnetic Particle Imaging. Int J Nanomed Nanosurg 2(3): doi http://dx.doi.org/10.16966/2470-3206.117

Abstract

Purpose: The purpose of this study was to quantitatively evaluate the tumor response to magnetic hyperthermia treatment (MHT) combined with radiation therapy (RT) in comparison with that to MHT alone using magnetic particle imaging (MPI).

Materials and methods: Colon-26 cells were implanted subcutaneously into the backs of 8-week-old male BALB/c mice. When the tumor volume reached approximately 100 mm^3, the mice were divided into a control (n=10), MHT (n=10), MHT+RT (n=8), and RT (n=7) groups. In the control group, neither MHT nor RT was performed. In the MHT and MHT+RT groups, the tumors were injected with magnetic nanoparticles (MNPs) (250 mM Resovist®) and were heated for 20 min using an alternating magnetic field (frequency: 600 kHz and peak amplitude: 3.1 kA/m). The mice in the MHT+RT and RT groups were irradiated to a dose of 7.5 Gy with a 4-MeV linear accelerator. In the MHT+RT group, MHT was performed 3 days after RT. In the MHT and MHT+RT groups, MPI images were obtained using our MPI scanner immediately before, immediately after, and 3, 7, and 14 days after MHT. After the MPI studies, we drew a region of interest (ROI) on the tumor in the MPI image and calculated the average, maximum, and total MPI values, and the number of pixels by taking the threshold value for extracting the contour of the tumor as 40% of the maximum MPI value (pixel value) within the ROI. Hematoxylin and eosin (H&E) stain images were also obtained in the MHT and MHT+RT groups immediately after and 7 days after MHT. In all groups, tumor volume *(V)* was measured every day and the relative tumor volume growth (RTVG) was calculated from $(V-V_0)/V_0$. In the control group, V_0 was taken as the tumor volume immediately after it reached approximately 100 mm^3. In the MHT and MHT+RT groups, V_0 was taken as the tumor volume immediately before MHT, whereas it was taken as the tumor volume 3 days after RT in the RT group.

Results: The RTVG value in the MHT+RT group was significantly lower than that in the control group 3 days or more after MHT and it was significantly lower than that in the MHT group 3 to 8 days and 11 to 14 days after MHT. Although the RTVG value in the MHT+RT group tended to be lower than that in the RT group, it did not reach statistical significance. The average MPI value in the MHT+RT group was significantly higher than that in the MHT group 3 and 7 days after MHT. The maximum MPI value in the MHT+RT group was significantly higher than that in the MHT group 3, 7, and 14 days after MHT.

Conclusions: Our results suggest that RT facilitates the retention of MNPs in the tumor in MHT and that MPI is useful for quantitatively evaluating the tumor response to not only MHT alone but also MHT+RT.

Keywords: Magnetic particle imaging; Magnetic hyperthermia treatment; Magnetic nanoparticles; Radiation therapy; Tumor response

Introduction

Magnetic particle imaging (MPI) is an imaging method that was introduced in 2005 [1]. MPI uses the nonlinear response of magnetic nanoparticles (MNPs) to an external oscillating magnetic field and is capable of imaging the spatial distribution of MNPs such as super paramagnetic iron oxide nanoparticles with high sensitivity and high spatial resolution [1].

Recently, we have developed an MPI scanner based on field-free-line encoding scheme [2,3] and succeeded in imaging the intratumoral distribution of MNPs and quantifying its temporal change *in vivo* [4,5]. We also showed that MPI is useful for predicting the therapeutic effect of magnetic hyperthermia treatment (MHT) [4,5].

MHT is one of hyperthermia treatments and employs the temperature rise of MNPs under an alternating magnetic field (AMF). MNPs generate heat through hysteresis loss and/or relaxational loss due to Nèel and Brownian relaxations when exposed to AMF [6]. Although conventional hyperthermia treatments such as radiofrequency (RF)-capacitive heating [7] damage not only tumor cells but also normal tissues, MHT can selectively heat tumor cells without damaging normal tissues [8]. In order to enhance the therapeutic effect of MHT, it is necessary to deliver and accumulate as many MNPs as possible into the tumor tissues [6]. Furthermore, the retention of MNPs in tumors is also one of the important factors to enhance the therapeutic effect of MHT [9]. When considering repeated applications of MHT, it is desired that MNPs are retained in the tumor for as long as possible.

Radiation therapy (RT) is one of traditional cancer therapies and irradiation has been reported to increase nanoparticle accumulation in tumors [10]. Thus, a combination of MHT and RT is expected to bring beneficial results [11].

This study was undertaken to quantitatively evaluate the tumor response to MHT combined with RT (MHT+RT) in comparison with that to MHT alone using MPI.

Materials and Methods

System for MPI

The details of our MPI system are described in our previous papers [2-5]. In brief, a drive magnetic field was generated using an excitation coil (solenoid coil 100 mm in length, 80 mm in inner diameter, and 110 mm in outer diameter). AC power was supplied to the excitation coil by a programmable power supply (EC1000S, NF CO., Yokohama, Japan), and was controlled using a sinusoidal wave generated by a digital function generator (DF1906, NF Co., Yokohama, Japan). The frequency and peak-to-peak strength of the drive magnetic field were taken as 400 Hz and 20 mT, respectively. The signal generated by MNPs was received by a gradiometer coil (50 mm in length, 35 mm in inner diameter, and 40 mm in outer diameter), and the third-harmonic signal was extracted using a preamplifier (T-AMP03HC, Turtle Industry Co., Ibaragi, Japan) and a lock-in amplifier (LI5640, NF Co., Yokohama, Japan). The output of the lock-in amplifier was converted to digital data by a personal computer connected to a multifunction data acquisition device with a universal serial bus port (USB-6212, National Instruments Co., TX, USA). The sampling time was taken as 10 msec. When measuring signals using the gradiometer coil, a sample was placed 12.5 mm (i.e., one quarter of the coil length) from the center of the gradiometer coil and the coil, including the sample, was moved such that the center of the sample coincided with the position of a field-free line. The selection magnetic field was generated by two opposing neodymium magnets (Neomax Engineering Co., Gunma, Japan). The field-free line can be generated at the center of the two neodymium magnets.

To acquire projection data for image reconstruction, a sample in the receiving coil was automatically rotated around the z-axis over 180° in steps of 5° and translated in the x-direction from -16 mm to 16 mm in steps of 1 mm, using an XYZ-axes rotary stage (HPS80-50X-M5, Sigma Koki Co., Tokyo, Japan), which was controlled using Lab VIEW (National Instruments Co., TX, USA). Data acquisition took about 12 min. Each projection data set was then transformed into 64 bins by linear interpolation. Both the inhomogeneous sensitivity of the receiving coil and feed through interference were corrected using the method described in the brief note by Murase et al. [12]. Transverse images were reconstructed from the projection data using the maximum likelihood-expectation maximization (ML-EM) algorithm over 15 iterations, in which the initial concentration of MNPs was assumed to be uniform [2,3].

Apparatus for MHT

The details of our apparatus for MHT are described in our previous paper [13]. In brief, the coil for generating the AMF consists of 19-turmed loops (6.5 cm in diameter and 10 cm in length) of copper pipe (5 mm in diameter) and cooled by water to ensure constant temperature and impedance. The coil was connected to a high-frequency power supply (T162-5723BHE, Thamway Co., Ltd., Shizuoka, Japan) and a manual-matching unit (T020-5723AHE, Thamway Co., Ltd., Shizuoka, Japan). This system can induce an AMF with maximum peak amplitude of 3.7 kA/m at an output power of 500 W. The peak amplitude of the AMF generated in the coil can be controlled by changing the output of the power supply.

Animal experiments using tumor-bearing mice

All animal experiments were approved by the animal ethics committee at Osaka University School of Medicine. Seven-week-old male BALB/c mice weighing 25.5 ± 1.2 g [mean ± standard deviation (SD)] were purchased from Charles River Laboratories Japan, Inc. (Yokohama, Japan), and were habituated to the rearing environment for one week before the experiment. The animals had free access to food and water and were kept under the condition of 23°C room temperature and around 50% humidity.

Colon-26 (a mouse cell line derived from rectal cancer) cells (Riken BioResource Center, Ibaragi, Japan) were cultured in RPMI-1640 medium (Mediatech Inc., VA, USA) supplemented with 10% fetal bovine serum (FBS) (Biowest, Nuaillé, France) and 1% penicillin-streptomycin (Nacalai Tesque Inc., Kyoto, Japan). All cultures were incubated in a humidified atmosphere containing 5% CO_2 at 37°C. The cells were trypsinized with 0.25% trypsin in ethylenediaminetetraacetic acid (EDTA) (Nacalai Tesque Inc., Kyoto, Japan) and resuspended in phosphate-buffered saline (PBS) at 1×10^6 cells/100 μL. The cells (1×10^6 cells) were implanted into the backs of eight-week-old male BALB/c mice (Charles River Laboratories Japan, Inc., Yokohama, Japan) on the same day and under the same conditions. During the implantation, the mice were anesthetized by intraperitoneal administration of pentobarbital sodium (Somnopentyl, Kyoritsu Seiyaku Co., Tokyo, Japan) (10-fold dilution, 0.012 mL/g body weight).

Magnetic nanoparticles

In this study, Resovist® (FUJIFILM RI Pharma Co., Ltd., Tokyo, Japan) was used as the source of MNPs, because it is commercially available and has been approved for clinical use in Japan [9]. Resovist® is an organ-specific contrast agent for magnetic resonance imaging, used especially for the detection and characterization of small focal liver lesions [13]. It consists of MNPs (maghemite, γ-Fe_2O_3) coated with carboxydextran.

Study protocol

When the tumor volume reached approximately 100 mm^3, the tumor-bearing mice were divided into a control (n=10), MHT (n=10), MHT+RT (n=8), and RT (n=7) groups.

In the control group, neither MHT nor RT was performed. The tumors in the MHT and MHT+RT groups were directly injected with Resovist® (0.2 mL of stock solution diluted in PBS) with an iron concentration of 250 mM, under anesthesia by intraperitoneal administration of pentobarbital sodium (Somnopentyl, Kyoritsu Seiyaku Co., Tokyo, Japan) (10-fold dilution, 0.012 mL/g body weight). After the injection of Resovist®, a mouse was placed in a plastic holder for undergoing MPI and MHT. MHT was started 20 min after the injection of Resovist® and was performed by applying an AMF at a frequency of 600 kHz and peak amplitude of 3.1 kA/m [13] for 20 min.

The MPI studies were performed five times for each mouse in the MHT and MHT+RT groups; immediately before MHT (2 min after the injection of Resovist®), immediately after MHT (42 min after the injection of Resovist®), and 3 days, 7 days, and 14 days after MHT.

After the second MPI study, X-ray CT images were obtained using a 4-row multi-slice CT scanner (Asteion, Toshiba Medical Systems Co., Tochigi, Japan) with a tube voltage of 120 kV, a tube current of 210 mA, and a slice thickness of 0.5 mm. The MPI images were co-registered to the X-ray CT images for anatomical identification using the method described in [4,5]. The X-ray CT images were also acquired 3 days, 7 days, and 14 days after MHT. It should be noted that the X-ray CT image after the second MPI study was substituted by that obtained after the first MPI study.

The mice in the MHT+RT and RT groups were irradiated to a dose of 7.5 Gy with a 4-MeV linear accelerator (Mitsubishi Electric Inc., Tokyo, Japan). The irradiation field size and source-surface distance (SSD) were 20×27 mm^2 and 100 cm, respectively. The 18-mm-thick lead sheet with a hole with a size of 17×13 mm^2 was used for the radiation shielding of the region except for the tumor. In the MHT+RT group, RT was performed 3 days before MHT as described above.

Histological study

Separately from the above studies, mice were purchased for histological studies and were implanted with colon-26 cells in the same manner as described above. When the tumor volume reached approximately 100 mm^3, the mice were divided into the MHT (n=3) and MHT+RT groups (n=3). The mice were sacrificed and the tumors were removed immediately after and 7 days after MHT.

The tumor tissues were fixed in 7.5% formaldehyde neutral buffered solution (Sigma-Aldrich Japan Co., Ltd., Tokyo, Japan) and were stained with hematoxylin and eosin (H&E). The histological images were acquired with a microscope (ECLIPSE80i, NIKON Co., Ltd., Tokyo, Japan) at 10x magnification and imaging software (NIS-Elements D, NIKON Co., Ltd., Tokyo, Japan).

Data and statistical analyses

The dimensions of the tumor were measured with a caliper every day and the tumor volume *(V)* was calculated from $V= (\pi/6) \times L_x \times L_y \times L_z$, where L_x, L_y, and L_z represent the vertical diameter, horizontal diameter, and height, respectively. The relative tumor volume growth (RTVG) was also calculated from $(V-V_0)/V_0$. In the control group, V_0 was taken as the tumor volume immediately after it reached approximately 100 mm^3. In the MHT and MHT+RT groups, V_0 was taken as the tumor volume immediately before MHT, whereas it was taken as the tumor volume 3 days after RT in the RT group. In this study, the RTVG value was used as an indicator of the therapeutic effect of MHT alone, MHT+RT, and RT alone.

We drew a region of interest (ROI) on the tumor in the MPI image and calculated the average, maximum, and total MPI values by taking the threshold value for extracting the contour of the tumor as 40% of the maximum MPI value within the ROI. In this study, the MPI value was defined as the pixel value of the transverse MPI image reconstructed from the third-harmonic signals. We also calculated the number of pixels within the ROI. It should be noted that the total MPI value is equal to the product of the average MPI value and the number of pixels.

The RTVG, average MPI value, maximum MPI value, total MPI value, and the number of pixels within the ROI were expressed as the mean ± standard error (SE). Differences in the RTVG value among groups were analyzed by one-way analysis of variance (ANOVA). Statistical significance was determined by Tukey-Kramer's multiple comparison tests. Differences in the average, maximum, and total MPI values and the number of pixels between the MHT and MHT+RT groups were analyzed by the Mann–Whitney U test. A P value less than 0.05 was considered statistically significant.

Results

Therapeutic effect

Figure 1 shows the time courses of the RTVG value in the control (red circles, n=10), MHT (blue squares, n=10), MHT+RT (green triangles, n=8), and RT groups (black diamonds, n=7). Although the RTVG value in the MHT group tended to be lower than that in the control group, it did not reach statistical significance. The RTVG value in the MHT+RT group was significantly lower than that in the control group 3 days or more after MHT and it was significantly lower than that in the MHT group 3 to 8 days and 11 to 14 days after MHT. Although the RTVG value in the MHT+RT group was slightly lower than that in the RT group, it did not reach statistical significance. The RTVG value in the RT group was significantly lower than that in the control group at 3 days or more.

MPI study

Figure 2 shows the typical examples of the MPI images superimposed on the X-ray CT images in the MHT+RT (upper row) and MHT groups (lower row), immediately before MHT and 3, 7, and 14 days after MHT. As shown in figure 2, the MPI pixel value decreased and the spatial distribution of MNPs changed with time in both groups. It was visually confirmed that the retention of MNPs in the tumor in the MHT+RT group was higher than that in the MHT group.

Figure 3 shows the temporal change of the average MPI value (a), maximum MPI value (b), total MPI value (c), and the number of pixels within the ROI (d) in the MHT+RT (red bars, n=8) and MHT groups (blue bars, n=10). The average MPI value in the MHT+RT group was significantly higher than that in the MHT group 3 and 7 days after MHT (Figure 3a). The maximum MPI value in the MHT+RT group was significantly higher than that in the MHT group 3, 7, and 14 days after MHT (Figure 3b). The total MPI value in the MHT+RT group tended to be higher than that in the MHT group 3, 7, and 14 days after MHT (Figure 3c). In contrast, the number of pixels within the ROI in the MHT+RT group tended to be lower than that in the MHT group 3, 7, and 14 days after MHT (Figure 3d). These tendencies, however, did not reach statistical significance.

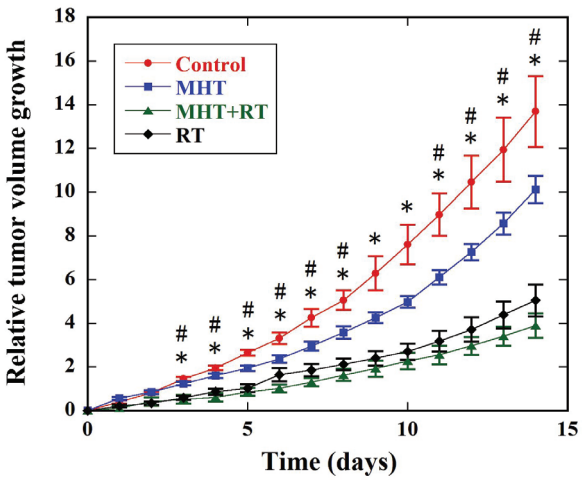

Figure 1: Relative tumor volume growth (RTVG) values in a control (red circles, n=10), MHT (blue squares, n=10), MHT+RT (green triangles, n=8), and RT groups (black diamonds, n=7). The mice in the control group underwent neither magnetic hyperthermia treatment (MHT) nor radiation therapy (RT). The mice in the MHT, MHT+RT, and RT groups underwent MHT alone, MHT combined with RT, and RT alone, respectively. ⁎: P<0.05 between the control and MHT+RT groups and between the control and RT groups, #: P<0.05 between the MHT and MHT+RT groups.

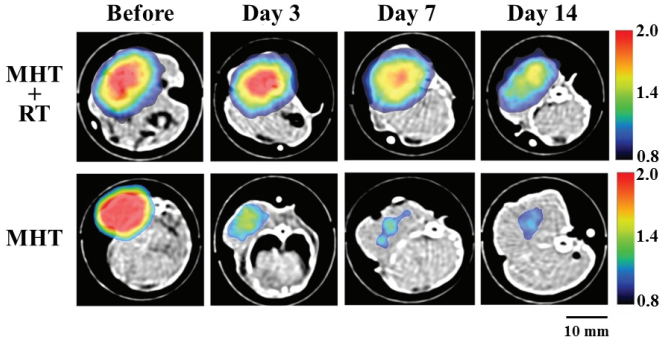

Figure 2: Images obtained by magnetic particle imaging (MPI) in the MHT+RT (upper row) and MHT groups (lower row) immediately before MHT and 3 days, 7 days, and 14 days after MHT. Note that the MPI images were superimposed on the X-ray CT images. Scale bar=10 mm.

Citation: Ohki A, Kuboyabu T, Aoki M, Yamawaki M, Murase K (2016) Quantitative Evaluation of Tumor Response to combination of Magnetic Hyperthermia Treatment and Radiation Therapy using Magnetic Particle Imaging. Int J Nanomed Nanosurg 2(3): doi http://dx.doi.org/10.16966/2470-3206.117

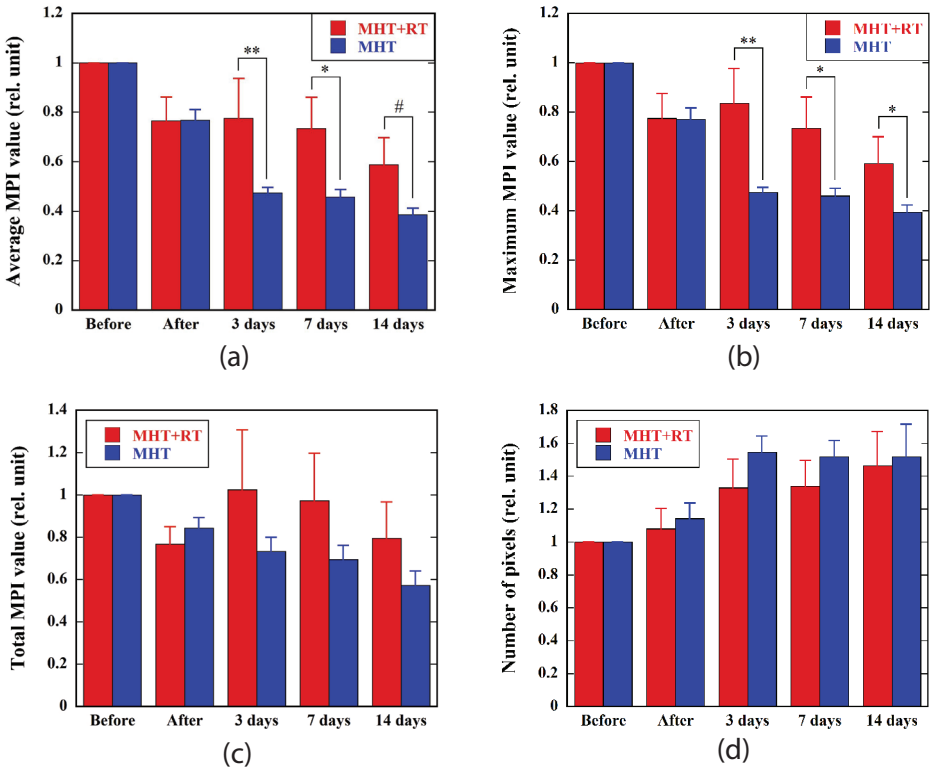

Figure 3: Average MPI value (a), maximum MPI value (b), total MPI value (c), and the number of pixels within the region of interest drawn on the tumor in the MPI image (d), immediately before, immediately after, 3 days, 7 days, and 14 days after MHT in the MHT+RT (red bars, n=8) and MHT groups (blue bars, n=10). Note that the values immediately after MHT and 3 days, 7 days, and 14 days after MHT were normalized by those immediately before MHT. Bar and error bar represent the mean and standard error, respectively. **: $P<0.01$, *: $P<0.05$, #: $P=0.055$.

Histological study

Figure 4 shows the typical H&E stain images in the MHT+RT (left column) and MHT groups (right column) immediately after (upper row) and 7 days after MHT (lower row). The necrotic area (shown by N) in the MHT+RT group was larger than that in the MHT group, whereas the viable area (shown by V) in the MHT+RT group was smaller than that in the MHT group.

Discussion

We quantitatively evaluated the tumor response to MHT combined with RT in comparison with that to MHT alone. As shown in figure 1, the RTVG value in the MHT+RT group was significantly lower than that in the MHT group 3 to 8 days and 11 to 14 days after MHT. Although there was a tendency for the RTVG value in the MHT+RT group to be lower than that in the RT group, it did not reach statistical significance (Figure 1). As previously described, MHT was started 20 min after the injection of 250 mM Resovist® and was performed by applying an AMF at a frequency of 600 kHz and a peak amplitude of 3.1 kA/m for 20 min. It is known that the absorption efficiency of MNPs to generate heat due to AMF depends on the frequency and peak amplitude of the AMF [6,13]. Atsumi et al. [14] used 600 kHz for the frequency in consideration of the safety and the capacity of their power supply. Thus, we also selected the above values for the frequency and peak amplitude in consideration of the safety, the capacity of our power supply, and the heating efficiency [13]. The duration of MHT (20 min) was determined mainly in order to prevent a mouse from awakening from anesthesia during the subsequent MPI study. In our previous study [4], when an AMF with the same frequency and peak amplitude as those in this study was applied to the tumor injected with 250 mM Resovist® for 20 min, the temperature in the tumor rose to around 40 to 42°C (mild hyperthermia). This temperature rise, however, might not be enough to get a statistically significant difference in the RTVG value between the MHT+RT and RT groups (Figure 1).

In this study, we investigated the temporal change of the MNPs injected into the tumor by calculating the average, maximum, and total MPI values and the number of pixels within the ROI drawn on the tumor in the MPI image, immediately before MHT, immediately after MHT, and 3, 7, and 14 days after MHT (Figure 3). We previously reported that there is an excellent linear correlation between the average MPI value and the iron concentration of Resovist® in phantom studies [4]. From this finding, it appears that the change in the average MPI value corresponds to that in the average amount of MNPs per voxel, i.e., the average concentration of MNPs, and the change in the total MPI value corresponds to that in the total amount of MNPs in the selected slice of the tumor, whereas the change in the number of pixels corresponds to that in the distributed area of MNPs. As shown in figure 3a, the average MPI value in the MHT+RT group was significantly higher than that in the MHT group 3 and 7 days after MHT. The maximum MPI value in the MHT+RT group was significantly higher than that in the MHT group 3, 7, and 14 days after MHT (Figure 3b). These findings are also visually confirmed by the MPI images shown in figure 2. Although the total MPI value in the MHT+RT group tended to be higher than that in the MHT group, it did not reach statistical significance due to large scattering of the data (Figure 3c). These results suggest that the MNPs injected directly into the tumor were confined to the tumor and their dispersion within the tumor and/or to the outside of the tumor was suppressed. Alternatively, they may suggest that the state of aggregation of MNPs in the tumor changed gradually due to irradiation. It has been reported that the diffusion of macromolecules into tumors is hindered because of the elevated interstitial fluid pressure (IFP)

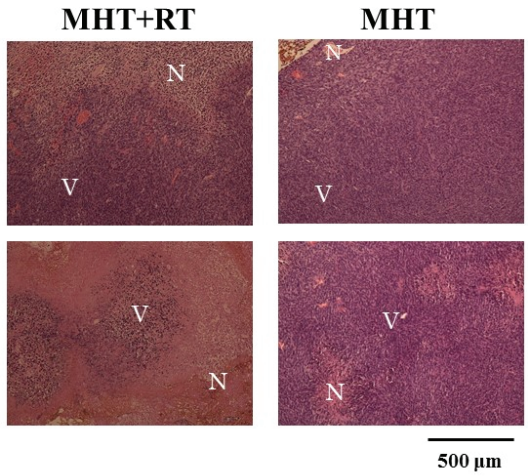

Figure 4: Hematoxylin and eosin (H&E) stain images in the MHT+RT (left column) and MHT groups (right column) immediately after (upper row) and 7 days after MHT (lower row). Magnification: × 10; N: Necrotic area; V: Viable area; Scale bar=500 µm.

in the tumor tissue [15] and irradiation reduces the IFP [10,16]. Thus, the above findings appear to be mainly due to the reduction in IFP induced by irradiation.

Giustini et al. [10] measured the IFP in the tumor by placing a fiber-optic pressure sensor in the centers of the tumors and reported that the IFP decreased gradually as compared with nonirradiated controls after the irradiation of a single 15-Gy fraction of 6-MeV electron radiation, became minimum 3 days after the irradiation, and increased gradually thereafter. Thus, in this study, we performed MHT 3 days after RT, at which the IFP in the tumor is supposed to become minimum from the above results of Giustini et al. [10].

Znati et al. [16] reported that a significant decrease in IFP was observed in female nude BALB/c mice implanted with the human colon adenocarcinoma LS174T for radiation doses of 10 Gy and 15 Gy, whereas a significant decrease in IFP was not observed for a radiation dose of 5 Gy. Thus, they concluded that a threshold for a decrease in IFP was 10 Gy of ionizing radiation [16]. When inspecting their data carefully, however, there was a tendency for the IFP to decrease even at 5 Gy. We speculate that a threshold for a decrease in IFP is lower than 10 Gy. When we irradiated tumor-bearing mice to a dose of 15 Gy, the therapeutic effect of RT alone was too strong and the synergistic effect of RT was masked when combined with MHT (data not shown). Thus, we adopted 7.5 Gy as a radiation dose for RT in this study.

Once MNPs are injected, MPI and MHT can be performed repeatedly until the MNPs disappear. The knowledge about the temporal change of the concentration and spatial distribution of MNPs in the tumor obtained by the repeated MPI studies will be useful for the treatment planning of MHT alone or MHT+RT. From the fact that RT enhances the retention of MNPs in the tumor (Figures 2 and 3), the combination of MHT and RT will be useful when considering the repeated application of MHT to enhance its therapeutic efficacy [17]. As shown by our previous studies [4,5], it would be necessary to quantify the amount of MNPs in the tumor accurately after the injection of MNPs for estimating the temperature rise in the tumor and thus for predicting the therapeutic effect of MHT alone or MHT+RT. When we design the optimal treatment planning of MHT alone or MHT+RT to prevent insufficient heating of the targeted region and overheating of the healthy tissue, accurate knowledge of the local concentration of MNPs accumulated in the targeted region appears to be important especially when the spatial distribution of MNPs is inhomogeneous.

A limitation of this study is that the MPI value was obtained from a single slice of the MPI image with the maximum signal intensity. Thus, the analysis with use of a single slice of the MPI image limits the accurate evaluation of the spatial distribution of MNPs in the whole tumor. For more detailed analysis, it will be necessary to acquire three-dimensional (multi-slice) data and to evaluate the three-dimensional distribution and accumulation of MNPs from these data. If this can be realized in the future, we expect that our MPI system can be used for more precise diagnosis and prediction of the therapeutic effect of MHT alone or MHT+RT and can be applied to theranostics, in which diagnosis and therapy are integrated in a single platform. In addition, we directly injected Resovist® into the tumor in this study; however, a method for active tumor-specific targeting of the MNPs injected intravenously should be established for clinical application. These studies are currently in progress.

Other methods for imaging MNPs are magnetic resonance imaging (MRI) and micro-CT imaging. When we attempted to image MNPs using MRI with a conventional transverse relaxation time (T_2*)-weighted imaging sequence, it was almost impossible due to large susceptibility-induced MR signal loss and image distortions in the regions near the MNPs especially for the high concentration of MNPs as is the case in MHT [3,4]. Recently, Dähring et al. [18] proposed the use of micro-CT for determining the MNP distributions within tumors and reported that the knowledge of the MNP distribution obtained by micro-CT enabled individualized MHT and improved the overall therapeutic efficacy. Although the use of micro-CT also appears to be promising and useful for establishing effective MHT, further studies especially on the accuracy and reproducibility in quantifying the amount of MNPs might be necessary for establishing the usefulness of the method.

Conclusion

In this study, we quantitatively evaluated the tumor response to MHT+RT in comparison with that to MHT alone using MPI. A significant difference in the RTVG value was not observed between the MHT+RT and RT groups under the present conditions of MHT and RT. However, the average MPI value in the MHT+RT group was significantly higher than that in the MHT group 3 and 7 days after MHT; the maximum MPI value in the MHT+RT group was significantly higher than that in the MHT group 3, 7, and 14 days after MHT, suggesting that RT facilitates the retention of MNPs in the tumor in MHT. Our results also suggest that MPI is useful for quantitatively evaluating the tumor response to not only MHT alone but also MHT+RT.

Acknowledgement

This work was supported by a Grant-in-Aid for Scientific Research (Grant Number: 25282131 and 15K12508) from the Japan Society for the Promotion of Science (JSPS).

Declaration of Interest

The authors report no conflicts of interest.

References

1. Gleich B, Weizenecker J (2005) Tomographic imaging using the nonlinear response of magnetic particles. Nature 435: 1214-1217.
2. Murase K, Hiratsuka S, Song R, Takeuchi Y (2014) Development of a system for magnetic particle imaging using neodymium magnets and gradiometer. Jpn J Appl Phys 53: 067001.

3. Murase K, Song R, Hiratsuka S (2014) Magnetic particle imaging of blood coagulation. Appl Phys Lett 104: 252409.

4. Murase K, Aoki M, Banura N, Nishimoto K, Mimura A, et al. (2015) Usefulness of magnetic particle imaging for predicting the therapeutic effect of magnetic hyperthermia. Open J Med Imaging 5: 85-99.

5. Kuboyabu T, Yabata I, Aoki M, Banura N, Nishimoto K, et al. (2016) Magnetic particle imaging for magnetic hyperthermia treatment: visualization and quantification of the intratumoral distribution and temporal change of magnetic nanoparticles *in vivo*. Open J Med Imaging 6: 1-15.

6. Kumar CS, Mohammad F (2011) Magnetic nanomaterials for hyperthermia-based therapy and controlled drug delivery. Adv Drug Deliv Rev 63: 789-808.

7. Abe M, Hiraoka M, Takahashi M, Egawa S, Matsuda C, et al. (1986) Multi-institutional studies on hyperthermia using an 8-MHz radiofrequency capacitive heating device (Thermotron RF-8) in combination with radiation for cancer therapy. Cancer 58: 1589-1595.

8. Petryk AA, Giustini AJ, Gottesman RE, Trembly BS, Hoopes PJ (2013) Comparison of magnetic nanoparticle and microwave hyperthermia cancer treatment methodology and treatment effect in a rodent breast cancer. Int J Hyperthermia 29: 819-827.

9. Kuboyabu T, Yamawaki M, Aoki M, Ohki A, Murase K (2016) Quantitative evaluation of tumor early response to magnetic hyperthermia combined with vascular disrupting therapy using magnetic particle imaging. Int J Nanomed Nanosurg 2: 1-7.

10. Giustini AJ, Petryk AA, Hoopes PJ (2012) Ionizing radiation increases systemic nanoparticle tumor accumulation. Nanomed 8: 818-821.

11. Horsman MR, Overgaard J (2007) Hyperthermia: a potent enhancer of radiotherapy. Clin Oncol 19: 418-426.

12. Murase K, Banura N, Mimura A, Nishimoto K (2015) Simple and practical method for correcting the inhomogeneous sensitivity of a receiving coil in magnetic particle imaging. Jpn J Appl Phys 54: 038001.

13. Murase K, Oonoki J, Takata H, Song R, Angraini A, et al. (2011) Simulation and experimental studies on magnetic hyperthermia with use of superparamagnetic iron oxide nanoparticles. Radiol Phys Technol 4: 194-202.

14. Atsumi T, Jeyadevan B, Sato Y, Tohji K (2007) Heating efficiency of magnetite particles exposed to AC magnetic field. J Magn Magn Mater 310: 2841-2843.

15. Jain RK, Stylianopoulos T (2010) Delivering nanomedicine to solid tumors. Nat Rev Clin Oncol 7: 653-664.

16. Znati CA, Rosenstein M, Boucher Y, Epperly MW, Bloomer WD, et al. (1996) Effect of radiation on interstitial fluid pressure and oxygenation in a human tumor xenograft. Cancer Res 56: 964-968.

17. Kawai N, Ito A, Nakahara Y, Honda H, Kobayashi T, et al. (2006) Complete regression of experimental prostate cancer in nude mice by repeated hyperthermia using magnetite cationic liposomes and a newly developed solenoid containing a ferrite core. Prostate 66: 718-727.

18. Dähring H, Grandke J, Teichgräber U, Hilger I (2015) Improved hyperthermia treatment of tumors under consideration of magnetic nanoparticle distribution using micro-CT imaging. Mol Imaging Biol 17: 763-769.